JOURNAL OF VIROLOGY, Oct. 2001, p. 9435–9445 Vol. 75, No. 19
0022-538X/01/$04.00+0 DOI: 10.1128/JVI.75.19.9435–9445.2001
Copyright © 2001, American Society for Microbiology. All Rights Reserved.

Cross-Linking of the Fingers Subdomain of Human Immunodeficiency Virus Type 1 Reverse Transcriptase to Template-Primer

ELENA N. PELETSKAYA,[1]† PAUL L. BOYER,[1]† ALEX A. KOGON,[1]† PATRICK CLARK,[2] HEIKO KROTH,[3] JANE M. SAYER,[3] DONALD M. JERINA,[3] AND STEPHEN H. HUGHES[1]*

ABL-Basic Research Program[1] and SAIC-Frederick,[2] National Cancer Institute at Frederick, Frederick, Maryland 21702-1201, and Laboratory of Bioorganic Chemistry, National Institute of Diabetes and Digestive and Kidney Diseases, National Institutes of Health, Rockville, Maryland 20892[3]

Received 12 December 2000/Accepted 29 June 2001

Cross-linking experiments were performed with human immunodeficiency virus type 1 (HIV-1) reverse transcriptase (RT) mutants with unique cysteine residues at several positions (positions 65, 67, 70, and 74) in the fingers subdomain of the p66 subunit. Two approaches were used—photoaffinity cross-linking and disulfide chemical cross-linking (using an oligonucleotide that contained an N^2-modified dG with a reactive thiol group). In the former case, cross-linking can occur to any nucleotide in either DNA strand, and in the latter case, a specific cross-link is produced between the template and the enzyme. Neither the introduction of the unique cysteine residues into the fingers nor the modification of these residues with photocross-linking reagents caused a significant decrease in the enzymatic activities of RT. We were able to use this model system to investigate interactions between specific points on the fingers domain of RT and double-stranded DNA (dsDNA). Photoaffinity cross-linking of the template to the modified RTs with Cys residues in positions 65, 67, 70, and 74 of the fingers domain of the p66 subunit was relatively efficient. Azide-modified Cys residues produced 10 to 25% cross-linking, whereas diazirine modified residues produced 5 to 8% cross-linking. Disulfide cross-linking yields were up to 90%. All of the modified RTs preferentially photocross-linked to the 5′ extended template strand of the dsDNA template-primer substrate. The preferred sites of interactions were on the extended template, 5 to 7 bases beyond the polymerase active site. HIV-1 RT is quite flexible. There are conformational changes associated with substrate binding. Cross-linking was used to detect intramolecular movements associated with binding of the incoming deoxynucleoside triphosphate (dNTP). Binding an incoming dNTP at the polymerase active site decreases the efficiency of cross-linking, but causes only modest changes in the preferred positions of cross-linking. This suggests that the interactions between the fingers of p66 and the extended template involve the "open" configuration of the enzyme with the fingers away from the active site rather than the closed configuration with the fingers in direct contact with the incoming dNTP. This experimental approach can be used to measure distances between any site on the surface of the protein and an interacting molecule.

Reverse transcriptase (RT) is the enzyme responsible for copying the single-stranded RNA genome of retroviruses into double-stranded DNA (dsDNA) (6, 37, 39). RT has two enzymatic activities: a polymerase that can copy either an RNA or a DNA template and an RNase H that can degrade RNA if (and only if) it is a part of an RNA-DNA hybrid. The RT of human immunodeficiency virus type 1 (HIV-1) is an important target for anti-HIV drugs; a number of the drugs approved for the treatment of HIV infections are RT inhibitors (27).

HIV-1 RT is a heterodimer composed of two subunits: The larger, p66, is 560 amino acids long, and the smaller, p51, contains the first 440 residues of p66 (6). The three-dimensional structure of HIV-1 RT has been solved. Three-dimensional structures that do and do not contain bound substrates and inhibitors have been quite helpful in understanding the functions of HIV-1 RT (8, 10, 11, 16, 21–26, 28, 31–33). The p66 subunit is composed of two domains: polymerase and RNase H. The polymerase domain contains the fingers, palm, and thumb subdomains; the connection subdomain links the polymerase domain to the RNase H domain. p51 is folded into similar subdomains (fingers, palm, thumb, and connection), but the relationships of those subdomains to each other are different in p66 and p51 (27, 29). We believe that a better understanding of the structure and function of HIV-1 RT might lead to the development of better drugs and drug therapies. However, a comparison of the available structures has made it clear that HIV-1 RT is quite flexible and that this flexibility plays an important role in the behavior of the enzyme. We do not yet understand how the enzyme moves when it changes between the states represented by the crystal structures; there is also the possibility that the flexibility of the enzyme allows it to assume states or structures that have yet to be discovered by either crystallographic or biochemical methods. We have used chemical cross-linking in an attempt to explore these possibilities. In the experiments reported here, we have focused on possible interactions between the fingers subdomain of the p66 subunit and the DNA substrate.

We have presented biochemical data to support the idea that the fingers subdomain of p66 interacts with an extended template (5) and, based on this evidence, proposed that such interactions can affect the positioning of the nucleic acid at the

* Corresponding author. Present address: HIV Drug Resistance Program, NCI-Frederick, P.O. Box B, Bldg. 539, Frederick, MD 21702-1201. Phone: (301) 846-1619. Fax (301) 846-6966. E-mail: hughes@ncifcrf.gov.

† Present address: HIV Drug Resistance Program, NCI-Frederick, Frederick, MD 21702-1201.

polymerase active site. This also led to the proposal that mutations in the fingers associated with resistance to nucleoside analog RT inhibitors acted by altering the position of the nucleic acid substrate relative to RT. The recent three-dimensional structure of a ternary complex of HIV-1 RT, a DNA template-primer, and a deoxynucleoside triphosphate (dNTP) shows that, in the presence of a dNTP, the fingers of p66 close, forming a dNTP binding pocket (25). This brings several of the amino acids in the fingers where there are mutations that are associated with nucleoside analog resistance in direct contact with the incoming dNTP. Hence, it is quite likely that these drug resistance mutations manifest themselves via direct interactions with the dNTP rather than indirectly through the DNA template. This new structure does not, however, explain the biochemical data which showed that template length had a significant effect on the ability of RT to incorporate nucleoside analogs (5). Nor does this structure rule out the possibility that there can be states and structures in which fingers of the p66 subunit interact with the extended template. The idea that there are interactions between HIV-1 RT and extended template is supported by observations that the efficiency of ternary complex formation is a function of template-primer size (36).

Our cross-linking experiments were performed with HIV-1 RT mutants that have unique cysteine residues introduced in several positions (positions 65, 67, 70, 74) in the fingers subdomain of the p66 subunit. Two approaches were used. In the first approach, a heterobifunctional photocross-linker was allowed to react with a specific cysteine in the fingers subdomain of p66. Essentially all of the SH groups were modified; this has little, if any, effect on the enzymatic activity of HIV-1 RT. DNA was allowed to bind to the modified mutant RT, and the complex was irradiated with UV light to activate the photocross-linker. In the second approach, an SH- linker was attached to specific positions in the DNA template (1). After the DNA was allowed to bind to RT, the ability of specific cysteine residue in the fingers of p66 to react with the SH in the DNA was measured. In the disulfide (S-S) chemical cross-linking experiments, defined chemical groups on RT and the DNA react. This reaction involves chemical entities that are minimally reactive to other chemical moieties, including buffer components and water. The efficiency of cross-linking is high, since there is no competition from other components in the reaction mixture. In contrast, photocross-linking is based on highly reactive species formed in situ by irradiation with UV light. The efficiency of the photocross-linking between DNA and protein is much lower than that of the SH-SH cross-linking reaction, because light-activated groups react with a wide range of compounds, including water and buffer components.

MATERIALS AND METHODS

Construction of mutant RT clones. By using *Bsp*MI cassette mutagenesis (4), an *Apa*I site was added to the p66 coding region of HIV-1 RT to make the construct RT (*Apa*I). This modification does not change the protein sequence of HIV-1 RT, but changes the codon usage at Pro52:

-GGG CCT GAG→-GGG CCC GAG-
Gly Pro Glu Gly Pro Glu

RT (*Apa*I) was modified to produce RT (Δ*Sca*I). In this plasmid, the HIV-1 RT coding region between codon 53 and codon 68 has been removed and replaced with a *Bam*HI site. RT (Δ*Sca*I) also has three new restriction endonuclease recognition sites created by site-directed mutagenesis: a *Sac*I site at codons 79 and 80 (—GAA CTT—to—GAG CTC—), a *Mun*I site at codons 91 and 92 (—CAA TTA—to—CAA TTG—), and an *Eco*RI site at codons 93 and 94 (—GGA ATA CCA—to—GGA ATT CCA—). None of these changes affects the protein sequence of HIV-1 RT.

To create the mutants K65C, D67C, K70C, and L74C, RT (Δ*Sca*I) was digested with *Apa*I and *Sac*I, and the large fragment was gel purified. Synthetic DNA fragments were generated by annealing complementary oligonucleotides. These synthetic DNA fragments span the region between codons 59 and 79 in the HIV-1 RT coding region and contain the codon changes to make the mutations K65C, D67C, K70C, and L74C. The synthetic DNA fragments have ends complementary to the overhangs created by *Apa*I and *Sac*I. The synthetic DNA fragments were ligated to the gel-purified *Sac*I-*Apa*I RT (Δ*Sac*I) DNA. The resulting plasmids were first analyzed by digestion with *Bam*HI (the desired clones do not have a *Bam*HI site) and then analyzed for the ability to express the p66 protein. Selected plasmids were then sequenced to prove the desired mutations were present.

The mutant C38V was constructed by using the clone RT (*Apa*I). RT (*Apa*I) was digested with *Sma*I and *Apa*I, and the DNA was gel purified. Synthetic oligonucleotides were annealed to generate a DNA fragment, which regenerates the *Sma*I site, encodes a valine residue at codon 38, and has an overhang complementary to the *Apa*I site. This synthetic DNA fragment was ligated to the *Sma*I-*Apa*I-digested RT (*Apa*I). The resultant clones were screened for the expression of the p66 protein and then sequenced to ensure the mutation was present.

The C38V mutation was introduced into plasmids carrying the K65C, D67C, K70C, and L74C mutations by using the *Apa*I site. The C38V plasmid was digested with *Apa*I-*Hin*dIII, and the 1,500-bp band was gel purified. The larger fragment from C38V and the smaller fragment from the K65C, D67C, K70C, and L74C mutants were ligated to generate the double mutant. Each of the double mutant plasmids was further modified to produce HIV-1 RT proteins containing the C280S mutation and six histidines at the C terminus. This gives plasmids in which the p66 coding region contains only a single cysteine residue at the designated location. The six-histidine tag at the C terminus of p66 aids in protein purification.

The expression vector pUC12N/p51(−cys) is similar to the coexpression vectors previously described (3). The vector contains two *lacZ* promoters oriented in opposite directions. One *lacZ* promoter transcribes a region encoding a p51 subunit with no cysteine residues (the specific mutations are C38V and C280S). The other *lac*Z promoter is oriented towards a polylinker, which contains a unique *Nco*I site and a unique *Hin*dIII site. The mutants described above, K65C(−cys)His, D67C(−cys)His, K70C(−cys)His, and L74C(−cys)His, were digested with *Nco*I-*Hin*dIII and cloned into pUC12N/p51(−cys). The resulting clones will coexpress the cysteine-less p51 subunit and a p66 subunit with a histidine tail and only one cysteine at the designated site.

Purification of HIV-1 RT. A single colony of *Escherichia coli* strain DH5α transformed with one of the plasmids mentioned above was inoculated into 750 ml of NZY medium and grown at 37°C for 12 to 14 h before harvesting by centrifugation. The expression system is based on pUC, so induction is not required for the production of HIV-1 RT. The bacterial pellet was washed once with Tris-buffered saline (TBS) (pH 7.5). The pellet was lysed and the RT was partially purified on a nickel-chelating affinity agarose column by using the six-His tag on the C terminus of p66. Pooled imidazole gradient fractions were dialyzed and then further purified on Q-Sepharose. Purity of the protein preparation was checked by denaturing polyacrylamide gel electrophoresis (PAGE).

Polymerase and RNase H assay. HIV-1 genomic sequences were subcloned from the pNL4-3 clone (2) into the LITMUS 28 plasmid (New England Biolabs, Beverly, Mass.) and sequenced. The R-PBS template RNA was synthesized according to the instructions contained in the Ambion Megashortscript kit (Ambion, Austin, Tex.). In brief, an oligomer containing a T7 promoter, modified so that it contained the correct sequence for the 5′ end of the R region (5′-TAC GCCAAGCTACGTAATACGACTCACTATAGGTCTCTCTGGTTAGACC AGATCTGAGCCTGGGA-3′), and a second oligomer containing the primer binding site (PBS) sequence (5′-AGTCCCTGTTCGGGCGCCA-3′) were used to generate a PCR fragment from the pNL4-3 sequence cloned into LITMUS. The PCR fragment was used as the template for RNA synthesis. RNA was purified by electrophoresis on a 5% denaturing gel and then visualized under UV light, and the 200-base base band was excised. The gel slice was soaked overnight in a solution of 50 mM Tris (pH 8.0) containing 400 μg of proteinase K per ml (Promega, Madison, Wis.). The supernatant was recovered, extracted three times with an equal volume of phenol-chloroform, and ethanol precipitated. RNA was quantitated using a UV spectrophotometer. DNA oligomers were labeled with [γ-^{32}P-]ATP (Amersham Pharmacia, Piscataway, N.J.) and T4 polynucleotide kinase (New England Biolabs).

R-PBS template RNA was mixed with a fivefold molar excess of [^{32}P]PBS (5′-AGTCCCTGTTCGGGCGCCA-3′) and and incubated at 37°C for 30 min. A threefold molar excess of RT was added to the annealed primer-template and allowed to bind for 1 min at 37°C. Synthesis was initiated with the addition of RT start solution containing dNTPs (80 μM final concentration) and $MgCl_2$ (6 mM final concentration). Reactions were stopped after appropriate incubation time by the addition of an equal volume of a 90% formamide stop solution containing 1% sodium dodecyl sulfate (SDS), 4 μg of plasmid DNA per ml, bromophenol blue, and xylene cyanole. Reaction mixtures were heated to 95°C for 4 min, fractionated by electrophoresis on a denaturing acrylamide gel containing 0.05% SDS, dried under vacuum, and exposed to a PhosphorImager screen (Molecular Dynamics, Sunnyvale, Calif.). The total amount of DNA synthesis was used as an indicator of polymerase activity. The RNase H assay was performed as described earlier (20), the only difference being that there was a twofold excess of RT in the reaction mixtures, which contained 100 nM RNA-DNA template-primer.

Oligonucleotides. Oligonucleotides were commercially synthesized by the phosphoroamidite method on a synthesizer with subsequent PAGE purification (BRL). Oligonucleotides were tagged by 5′ labeling with [γ^{32}P]ATP with T4 polynucleotide kinase (T4 PNK) obtained from Boehringer Mannheim and annealed at a 1:1 ratio for cross-linking experiments.

Oligonucleotide synthesis with 8-amino-3,4-dithiaoctyl tether at N^2 of dG. The oligonucleotide 30-mer 5′-GTG TGT GT[FdI] ATC GTG GCG CCC GAC AGG GAC-3′ was prepared on commercial dC-cpg (40 to 50 μmol/g) with a standard synthesizer protocol for generation of the 21-base sequence at the 3′ end. The 5′-DMT (dimethoxytrityl chloride)-protected phosphoramidite (15) derived from O^6-(2-*p*-nitrophenylethyl)-2-fluoro-2′-deoxyinosine was coupled manually to the 5′ end of the oligonucleotide bound to the support (7). A typical 2-μmol synthesis utilized 20 mg (21 μmol) of the phosphoramidite and 150 μl of 0.5 M 4,5-dicyanoimidazole in acetonitrile for 16 h at room temperature; yield was estimated from the recovery of DMT cation after deprotection. End capping with acetic anhydride was omitted after the manual coupling step (7), and the support-bound oligonucleotide was directly oxidized (1 M tetrabutyl hydroperoxide in dichloromethane for 30 s) and returned to the synthesizer for addition of the remaining eight residues by the standard automated synthesis procedure. After removal of the 5′-DMT protecting group, the linker was coupled to the support-bound oligonucleotide by a modification of the procedure of Erlanson, Chen, and Verdine (15). The support-bound oligonucleotide was treated with a combination of 45 mg (178 μmol) of 3,3′-dithiobis(propylamine) dihydrochloride (17), which was prepared as described for the 4-carbon homolog (12), 60 μl (600 μmol) of triethylamine, and 100 μl of H_2O for 16 h at room temperature. In the course of preparing O^6-(2-*p*-nitrophenylethyl)-2-fluoro-2′-deoxyinosine, we observed cleavage of the nitrophenylethyl protecting group in the presence of wet *tert*-butyl ammonium fluoride. After reaction with dithiobis(propylamine), addition of concentrated NH_4OH (1.5 ml) containing 20 μmol of *tert*-butyl ammonium fluoride to the beads and solution, followed by heating at 60°C for 3 days, resulted in complete deblocking of the oligonucleotide; this procedure avoided the DBU (1,8-diazabicyclo[5.4.0]undec-7-ene)-formamide cleavage step and accompanying formylation (15) of the free amino group of the tether. After filtration, the oligonucleotide solution was dialyzed against 0.1 M triethylammonuim acetate buffer (pH 6.0) overnight to remove excess amines. The oligonucleotide was purified by high-performance liquid chromotography on a Hamilton PRP-1 column (7 μm, 10 by 250 mm) eluted at 3 ml/min with a linear gradient of acetonitrile in 0.1 M $(NH_4)_2HCO_3$ buffer (pH 7.5) which increased the acetonitrile concentration from 0 to 17.5% over 20 min (retention time, 16.3 min). Mass spectrometry (electrospray) calculated, 9,477; found, 9,475.

Photoaffinity cross-linking. Ideally, photoaffinity cross-linking is performed by using a reagent that is covalently attached to one of the members of a biomolecular complex (here, RT), and this reagent remains inert to all components of the reaction mixture until it is activated by irradiation with mild UV light. Photoactivation is initiated only after the relevant biomolecular complex has formed, and activation transforms the reagent into a highly active and (presumably) highly unselective chemical moiety that quickly reacts with its nearest neighbor whether it is a part of a biomolecular complex, a buffer component, or a water molecule. If there is a specific complex, the probability of cross-linking to the other component of the biochemical complex (in this case, DNA) is significantly higher than if there is no such complex. Even though nonspecific reactions with other components of the mixture (primarily water) reduce the efficiency of the cross-linking to DNA, the nonselectivity of the reaction means that the photocross-linking of two biological components (RT and DNA) can be interpreted as a direct interaction, and the shortest distance between the two cross-linked points in the natural complex can be considered to be no greater than the length of the cross-linker.

Photocross-linkers. We used two types of photoactivatable thiol-specific reagents: a carbene-generating compound, *N*-bromoacetyl-*N*′-{2,3-dihydroxy-3-[3-(3-(trifluoromethyl)diazirin-3-yl)phenyl]propionyl}ethylenediamine (BATDHP), obtained from Biolinx LLC (Hagerstown, Md.) and a nitrene-generating compound, azidophenacylthiopyridine (APTP), obtained from Sigma (St. Louis, Mo.) (29). These were coupled to the SH- group of single Cys-containing RT mutants. Carbenes are among the most reactive moieties known. They are capable of reacting with any chemical bond present in a biomolecule, including aliphatic chains and aromatic rings. Reacting in nanoseconds, carbenes rapidly form covalent bonds with neighboring atoms. The significant electrophilicity of carbenes is "overpowered" by their high reactivity, and, in the absence of nucleophiles, carbenes will react even with C-H bonds (over 80% cross-linking to cyclohexane (35, 38). The high level of reactivity of carbenes with buffer components usually precludes high yields of cross-linked products.

Nitrenes, such as those generated from the azide-containing reagent APTP, are less reactive and tend to undergo intramolecular rearrangements that lead to less reactive products. They cross-link primarily to nucleophiles such as amino groups and, in a nonnucleophilic environment, can remain active for periods of up to several minutes. This makes them less reliable for the detection of close interactions, since selective cross-linking may occur to a relatively distant nucleophilic group that is only occasionally in the vicinity of the cross-linker. The efficiency of cross-linking with nitrenes formed from azides is thus higher, but there is a possibility of bias toward interactions with nucleophilic groups. Photocross-linking reagents were prepared as 10 to 20 mM stock solutions in dimethyl sulfoxide and stored in the dark at −20°C for not longer than 30 days.

RT modification. All of the RT mutants were modified with photocross-linking reagents via a single Cys residue on p66. Fifty microliters of 1 to 10 μM solutions of RT were treated with 5 mM DTT on ice for 30 min to reduce the SH- group. DTT was than removed by gel filtration with Centrisep desalting columns (from Princeton Separations, Adelphia, N.J.) in buffer 1 (Tris-Cl [pH 8.0] 60 mM KCl, 10 mM $MgCl_2$, 1 mM CHAPS {3-[(3-cholamidopropyl)-dimethylammonio]-1-propanesulfonate}). The reduced RT was allowed to react with 10- to 50-fold molar excess of a photoreagent in dark vials on ice for 4 to 12 h. Excess of the photocross-linking reagent was removed by gel filtration. All subsequent manipulations were carried in low light levels.

To estimate the extent of SH-modification, RT samples were reacted (before and after modification with thiol-specific cross-linking reagents) with thiol-specific biotin-maleimide (BMCC) from Pierce (Rockford, Ill.) at pH 5.2 according to the manufacturer's instructions. All of the reactions were performed in degassed buffers under argon gas. Samples were loaded on nonreducing PAGE in 1 M SDS and 3 M urea without boiling to avoid non-thiol-specific biotinylation at high pH and high temperatures. Reaction mixtures were analyzed by Western blotting with streptavidin conjugated to alkaline phosphatase from Sigma (St. Louis, Mo.).

Photocross-linking reactions. Modified RT (1 μM) and template-primer (0.03 μM [5′ labeled with [γ^{32}P]ATP]) were incubated in buffer 1 for 5 min at 37°C and then UV irradiated with a handheld lamp (model UVM-57 from UVP, Upland, Calif.) for 15 min on ice with a glass plate as an additional filter (cutoff, 315 nm). Nonreducing denaturing PAGE was used for separation of the template-primer covalently cross-linked to RT. The cross-linked products were quantified with a PhosphorImager (Storm 860 from Molecular Dynamics, Inc., Sunnyvale, Calif.). The negative control samples were obtained by cleaving specific covalent bonds in the cross-links. APTP cross-links can be cleaved by reducing the disulfide bond formed with the SH group of modified Cys. BATDHP cross-links are cleavable in the presence of 10 mM $NaIO_4$ which oxidizes a *cis*-diol bond built into the reagent for this purpose.

Chemical cross-linking. The chemical cross-linking experiments were designed so that the reaction (S-S cross-linking) involved a particular chemical group on both biomolecules (RT and DNA). The reagents have only a minimal reactivity to other chemical moieties, including buffer components and water. Since there are no other targets in the reaction mixture, this type of chemical cross-linking is efficient. Unlike photoactivatable reagents, the chemical cross-linkers are reactive during the whole time of an experiment. This means cross-linking can occur whenever the modified elements are close enough for interaction, which does not necessarily require that these elements be appropriately complexed. However, in experiments in which an SH- group on DNA was cross-linked to the thumb of HIV-1 RT, cross-linking was specific and depended on appropriate alignment of the SH- groups on the protein and the nucleic acid (25).

The reaction mixture containing 0.03 μM template-primer with 1 to 2 μM RT in buffer 1 was incubated for various times up to 2 h at 37°C (Table 1). This assay was also performed with template oligonucleotides 5′- labeled with γ-^{32}P. Excess RT was present in the reaction mixture to ensure that all of the cross-linking

TABLE 1. Oligonucleotide pairs used in SH-cross-linking experiments

Template or primer	Sequence[a]
Template	5′-GTGTGTGTG*ATCGTGGCGCCCGACAGGGAC-3′
Primer 1	3′-CCGCGGGCTGTCCCTG-5′
Primer 2	3′-ACCGCGGGCTGTCCCTG-5′
Primer 3	3′-CACCGCGGGCTGTCCCTG-5′
Primer 4	3′-AGCACCGCGGGCTGTCCCTG-5′

[a] G* is the modified nucleotide.

occurs in RT bound to template-primer. The products were fractionated by nonreducing denaturing PAGE and quantified with a PhosphorImager. The disulfide bonds in the cross-linked products were cleaved to produce the negative control samples.

RESULTS

HIV-1 RT mutants were created that had the cysteines normally present at positions 38 and 280 replaced (by valine and serine, respectively) and also had a single cysteine residue introduced into specific positions of the p66 fingers subdomain. The unique Cys residues in each mutant were modified with one of the two thiol-reactive heterobifunctional photocross-linking reagents—APTP (azide) or BATDHP (diazirine). These modified RTs were allowed to bind to dsDNA template-primer. Upon irradiation with mild UV light (maximum absorbances of the photocross-linking reagents are 320 and 366 nm, respectively), the photoactivatable groups rapidly and nonspecifically form covalent bonds with any molecule within range. Since the reactive state of the cross-linker is extremely short-lived, it can only form covalent bonds with moieties that are in close proximity to the photoactivated group when the cross-linker is activated. This property ensures that only direct interactions are detected and that distances between the parts of biomolecules that are cross-linked in the reaction do not exceed the size of the cross-linker. We have used reactivity with maleimide biotin to demonstrate that the reactive SH- group of the various RT mutants was fully modified (Fig. 1). The polymerase and RNase H activities of the mutant enzymes were similar to those of wild-type HIV-1 RT both before and after modification with photoaffinity reagents (data not shown).

Cross-linking to template and primer strands. There was relatively efficient photoaffinity cross-linking of template-primer with a template that had an 11-nucleotide (nt) 5′ overhang and the modified RT proteins with Cys residues in positions 65, 67, 70, and 74 of the fingers domain of the p66 subunit. The relationship of the b3-b4 loop with template-primers and the scheme of the reactions are shown in Fig. 2. APTP-modified RTs produced 10 to 25% cross-linking, BATDHP-modified RTs produced lower yields of cross-linking (<8%). This is consistent with the chemical properties of the carbene-generating photocross-linker. Relative to APTP, BATDHP has a longer spacer (12 Å), and the reactive species has a shorter half-life (10^{-9} s). These results suggest that RT residues 65, 67, 70, and 74 are all located within 7 to 12 Å of the template-primer. Relative levels of cross-linking with the same template-primer are similar for modified cysteines at positions 65, 67, and 74 (up to 25% with APTP and 5 to 8% with BATDHP) and lower for position 70 (6 and 2%), respectively.

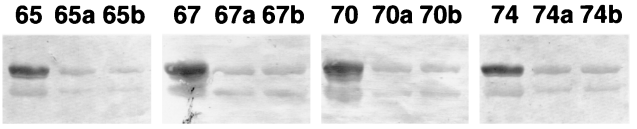

FIG. 1. Thiol-selective biotinylation of single cysteine residues in mutant RTs before and after modification with photocross-linkers. Biotinylation was visualized by Western blotting. Equal amounts of proteins were loaded on a gel in each lane. 65, K65C; 67, D67C; 70, K70C; 74, L74C; a, APTP; b, BATDHP.

In order to determine which strand of the template-primer reacted with the photoaffinity reagent, we used template-primer duplexes in which either the 5′ end of the template or the primer was labeled. In these experiments, we used templates with an 11-nt 5′ overhang. To avoid the possibility of partial denaturation of dsDNA in a protein gel (which would overestimate the amount of cross-linking to the labeled strand), we used both a nonreducing protein gel and a Tris-borate-EDTA–urea 6% denaturing sequencing gel to determine the extent of cross-linking. All of the mutant RTs preferentially photocross-linked to the template strand of the dsDNA template-primer substrate. Formation of cross-links with the primer strand was about 5- to 10-fold less efficient for APTP and 3- to 8-fold lower for BATDHP reagent than cross-links to the template strand (Fig. 3). These experiments were also performed with different lengths of the template overhang, and similar results were obtained even if the template overhang was as short as +2 (data not shown).

Having established that the cross-linking primarily involved the template strand for the four different sites in the fingers subdomain, protein gels were used for subsequent analysis, and we assumed that cross-linking to the primer strand was only a minor portion of the total cross-linking.

Different template overhangs. Experiments comparing the efficiency of cross-linking with template overhangs of various lengths made it possible to estimate the preferred position of cross-linking to the template. The template overhang sequence was a (TG)n repeat that should have no propensity to form secondary structures and no heterogeneity in sequence. Assuming that the probability of cross-links to an extended template is a function of the spatial position of the individual amino acid residues relative to template overhang and not a function of the nucleotide sequence of DNA, these data can be used as a measure of distance between the defined mutant Cys and the position on the template. Since the photocross-linkers are on flexible arms and have no strong specificity for distinct positions along the templates we have used, cross-linking to a longer template will always be as efficient as, and will often be more efficient than, cross-linking to a shorter template. As might be expected, the efficiency of cross-linking plateaued as the template was extended. This allows us to estimate the range of template lengths for which the photocross-linkers make optimal contacts with the nucleic acid. By using two photocross-linkers with different chemistry, we should be able to obtain unambiguous results (Fig. 4). The data presented in Fig. 4 are normalized for convenience of comparison and to enable averaging of multiple independent experiments that

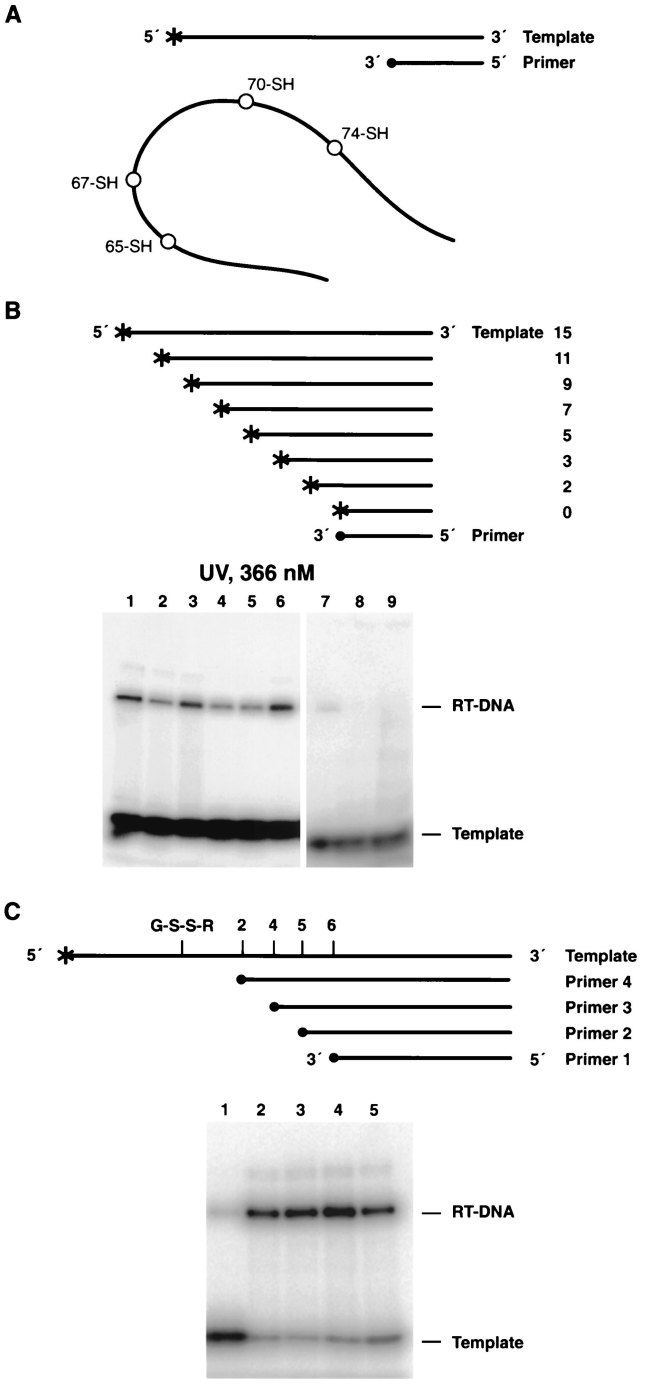

FIG. 2. Photoaffinity cross-linking and chemical cross-linking. (A) Appropriate relationship of the β3-β4 loop that carries the cysteine substitutions at positions 65, 67, 70, and 74 and the template-primer. In the diagram, the end of the extended template is ^{32}P labeled (*). (B) In the photocross-linking experiments, templates with different extensions (0 to 15) were each annealed to the same primer. Modified RTs were incubated with template-primer with an 11-nt extension (TP11) and cross-linked (366 nm). The cross-linked samples were fractionated on an SDS-polyacrylamide gel (4 to 20% polyacrylamide). Lanes: 1, K65C-APTP; 2, K65C-BATDHP; 3, D67C-APTP; 4, D67C-BATDHP; 5, L74C-BATDHP; 6, L74C-APTP; 7, K65C-APTP with TP11 without UV treatment; 8, K65C-APTP cross-linked to TP11 and subsequently cleaved with DTT; 9, K65C-BATDHP cross-linked to TP11 and subsequently cleaved with 10 mM $NaIO_4$. (C) For chemical cross-linking, a single template containing modified G (G-S-S-R) was ^{32}P labeled (*). These template-primers were allowed to react with mutant HIV-1 RTs containing a cysteine residue and were fractionated by nonreducing PAGE. Lanes: 1, K65C with template-primer 2 (TP2) and subsequently cleaved with DTT; 2, K65C+TP4; 3, K65C+TP3; 4, K65C+TP2; 5, K65C+TP1.

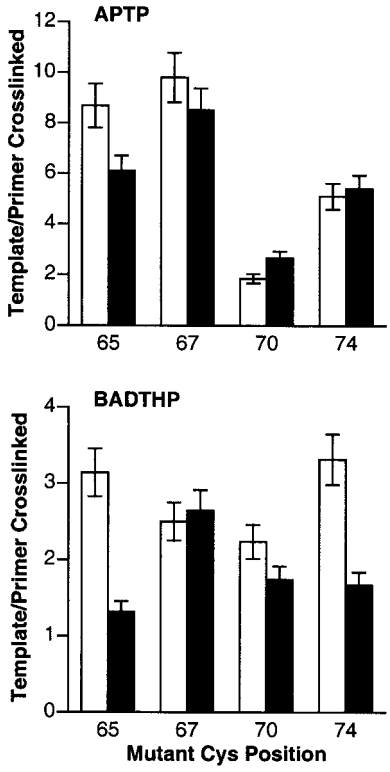

FIG. 3. Photocross-linking efficiency of template and primer strands. The ratio was calculated as follows: % crosslinking to template/% cross-linking to primer. Tris-borate-EDTA (6%)–urea gels were used to fractionate the reaction products. The average of five independent experiments is plotted, and error is calculated as standard deviation. □, −dNTP; ■, +dNTP.

had similar patterns, but the absolute values obtained in the experiments varied. The actual yields of cross-linking at maximum (generally with TP+11) were as follows:

K65C-APTP, 15% ± 3%; K65C-BATDHP, 4% ± 2%
D67C-APTP, 20% ± 5%; D67C-BATDHP, 4% ± 2%
K70C-APTP, 7% ± 3%; K70C-BATDHP, 2% ± 1%
L74C-APTP, 25% ± 8%; L74C-BATDHP, 5% ± 2%.

The results obtained with the two cross-linkers are similar. For positions 65 and 70, the results obtained with BATDHP and APTP are offset by about 2 bases, which could reflect the difference in the length of the cross-linking arms. However, these differences are less obvious for positions 67 and 74. Modified RTs with photocross-linkers at positions 65 and 74 of p66 demonstrate significant cross-linking with template overhangs of +5 and longer. No additional increase in cross-linking occurs after +7 for K65C, and there is little increase beyond position +5 for L74C. The corresponding range for D67C is +7 to 11, and for K70C, it is +5 to 11. (Fig. 4). Comparing the

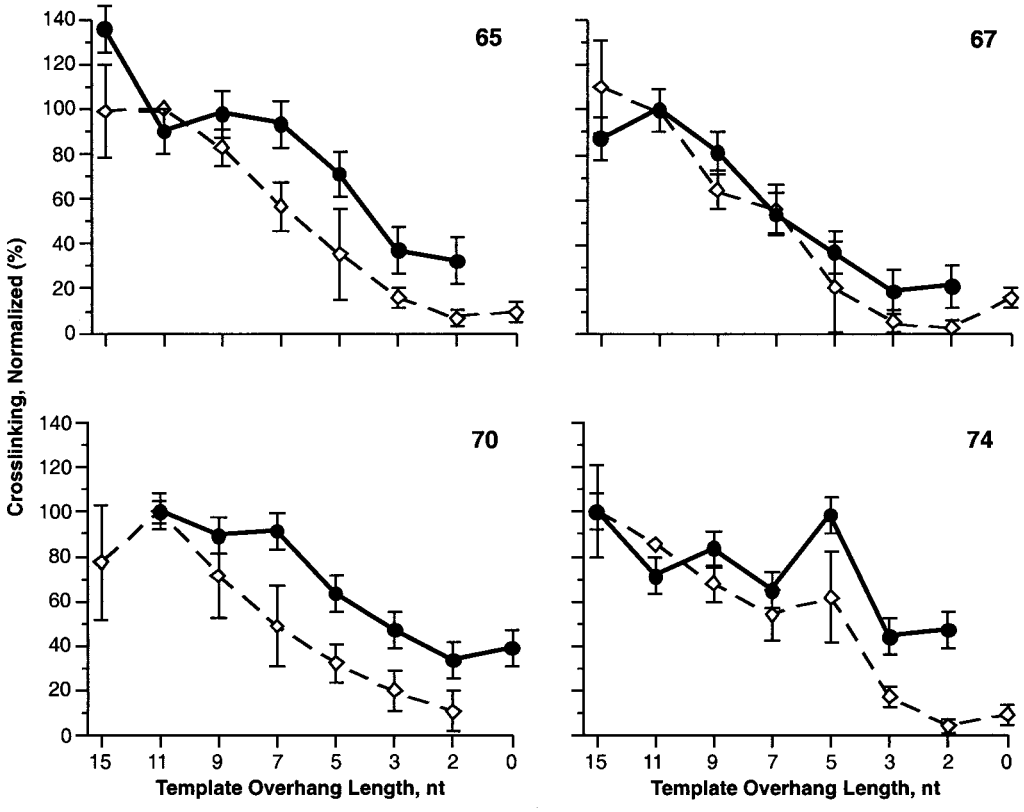

FIG. 4. Yield of photocross-linking as a function of template extension length. The average of seven independent experiments is plotted, and error is calculated as standard deviation. 65, K65C; 67, D67C; 70, K70C; 74, L74C. ◇, APTP; ●, BATDHP.

efficiency of cross-linking suggests that the path taken by the DNA template extension beyond polymerase active site first passes by position 74, then passes 65 and 70, and finally goes past 67.

Effects of dNTP binding. Crystallographic studies have shown that binding of an incoming dNTP to the DNA-RT complex alters the position of the p66 fingers subdomain (25). We wanted to study the effect of this type of structural change on photocross-linking to the extended template. To avoid incorporation of the incoming dNTP, experiments were performed with ddG at the 3′ end of the primer. Addition of a dNTP mix (100 μM each) to such RT-DNA complexes leads to the formation of a stable ternary complex with the incoming dNTP (19, 25, 36). Because the modified RTs retain full polymerase activity, we have assumed that they bind the incoming dNTP normally. The addition of 100 μM dNTPs to complexes formed with any of the modified RTs affects the efficiency of the photocross-linking reactions. To help understand how binding a dNTP affects the efficiency of photocross-linking, the results of experiments done with and without dNTP were compared. To be sure that there is no alteration of template-primer preference, experiments were done to determine the relative efficiency of the cross-linking to the template and the primer. In the presence of the incoming dNTP, the preference for cross-linking to the template is not affected for position 67, there is moderate decrease for position 70, and there a more significant decrease for positions 65 and 74 (see Discussion). In terms of efficiency of cross-linking, there was in general more cross-linking in the open configuration. However, when the template overhang was short, cross-linking was low, but there was more cross-linking with the closed configuration (Fig. 5). These results are entirely consistent with what we know about the structure of the open and closed complexes. When the template extension is short, the closed conformation would bring the photocross-linker closer to the DNA, which would allow for some cross-linking to occur. However, when the template extension is long, the closed configuration could interfere with the ability of the fingers to interact with the extended template.

SH-cross-linking. A chemically modified oligonucleotide was synthesized that contained an SH- tether linked at the N^2 of guanine residue at a defined position of the template (Materials and Methods). The SH-modified template oligonucleotide was 5′- labeled and annealed with one of the primers that placed the modified guanine at a specific position on the template. By adding appropriate dNTPs and/or ddNTPs, these primers were extended by RT to change the position of the modified G* residue relative to the active site as desired and create either a binary complex (RT-DNA) or a ternary complex (RT-DNA-NTP). In the absence of a reducing agent, disulfide bonds can form if the free SH- groups of the protein and DNA are in close contact (25). The relative efficiency of such cross-linking was used as a measure of the relative positions of the two SH- groups (one on the DNA template over-

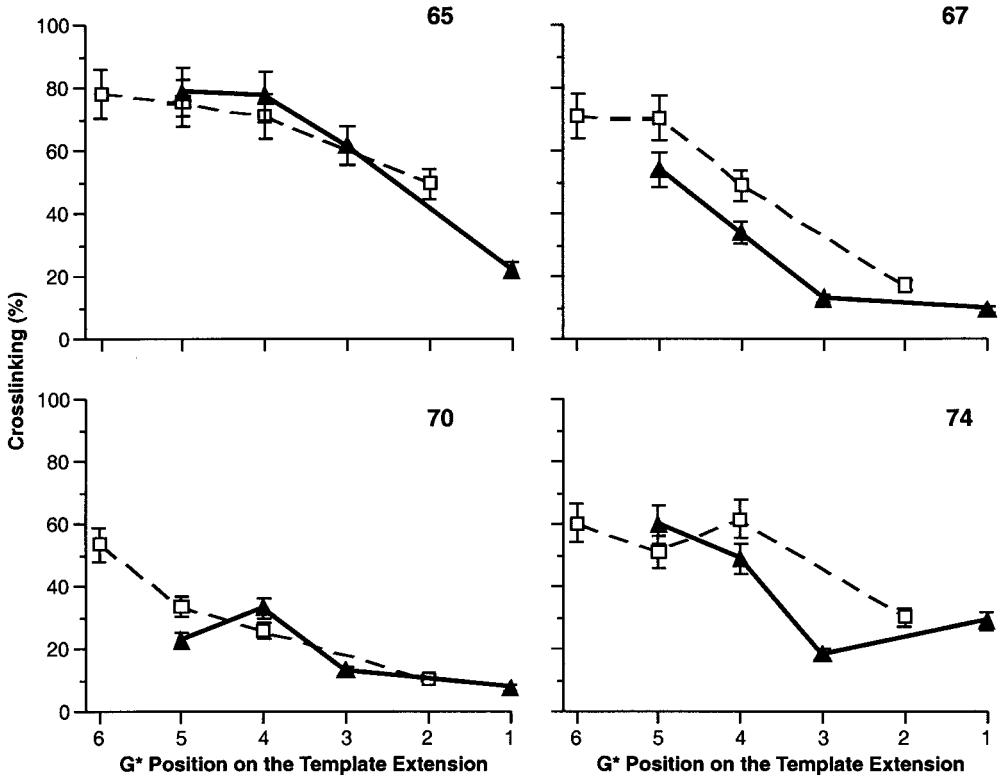

FIG. 5. Relative percent change of the yield of photocross-linking in binary and ternary complexes of RT with various template extension lengths. The relative yield was calculated as follows: [(cross-linking in binary complex − cross-linking in ternary complex)/cross-linking in binary complex)] × 100. The average of multiple independent experiments is plotted, and error is calculated as standard deviation. 65, K65C; 67, D67C; 70, K70C; 74, L74C. □, APTP; ■, BATDHP.

hang and the other on RT). To ensure that the cross-linking occurred only as a result of direct interaction, RT was used in molar excess relative to the modified template-primer. The cross-linking kinetics demonstrated that no measurable cross-linking occurred before 5 min, by which time all of the template-primer was bound and extended by RT (data not shown). The length of the tether connecting the sulfhydryl group to guanine was used as a measure of distance (≤4 Å) between two cross-linked points. This provided an independent measure of distance that could be compared with the photoaffinity cross-linking experiments. No RT-RT crosslinking was seen, which suggests that the cross-linking to the nucleic acid was specific (data not shown).

All of the mutant Cys residues (positions 65, 67, 70, and 74) reacted with the sulfhydryl group on the modified template. The cross-linking yields are as high as 80% for K65C, L74C, and D67C and 30 to 40% for K70C. These data suggest that the template-primer and the fingers of RT can interact in a fashion that puts the two sulfhydryls in close proximity and at appropriate angles.

To determine the position of the nearest nucleotide residue on the template overhang that can form a disulfide bond with the thiol group of the mutant RT, we performed a number of cross-linking experiments with the modified template annealed with DNA primers of various lengths. When binary complexes were formed with K65C and L74C, the optimal SH-cross-linking was observed at positions +4 to 5, while for D67C and K70C, the preferred positions were +5 to 6 relative to polymerase active site (Fig. 6). This is in reasonable agreement with the photoaffinity cross-linking experiments.

As has already been discussed, the position of the fingers changes when HIV-1 RT binds an incoming dNTP. To determine how differences in the position of the fingers affects cross-linking, ternary complexes (RT-DNA-NTP) were formed with primers of various lengths by addition of complementary ddNTP and then dNTP (100 μM each). The relative efficiency of SH cross-linking to the modified G* in binary complexes was slightly higher than in ternary complexes (Fig. 7). There was no shift of the preferred position of cross-linking for K65C and K70C cross-linking; for D67C and L74C, the preferred position was shifted 1 base farther away (from +4 to +5).

DISCUSSION

Published data and the data presented here demonstrate that site-directed cross-linking can be used to measure distances between any site on the surface of a protein and an interacting molecule. Most of the photoaffinity studies of protein-nucleic acid interactions were performed with modified nucleic acids (see reference 18 for a review of applications of thionucleobases). It is often difficult to map the sites of cross-linking on protein by partial protease digestion and amino acid analysis and/or mass spectrometry. Introduction of modified nucleotides could cause artifacts in the interactions with pro-

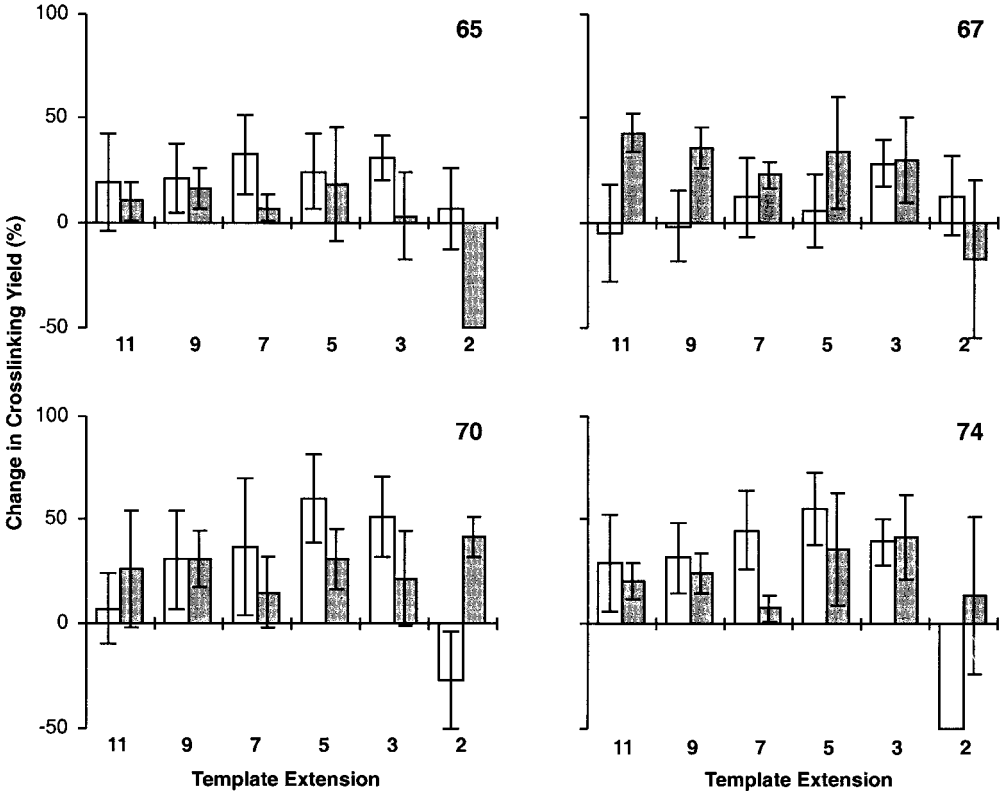

FIG. 6. Yield of SH-cross-linking as a function of template extension length in binary and ternary complexes of RT. The average of five independent experiments is plotted, and error is calculated as standard deviation. 65, K65C; 67, D67C; 70, K70C; 74, L74C. □, binary complex; ▲, ternary complex.

teins. Site-directed mutagenesis can be used to introduce cysteines at specific sites in the protein; the cystines can then be modified with cross-linking agents. This approach has been used to study the interactions of nucleic acids with several proteins, including LexA (13, 14), PKR (RNA-dependent protein kinase) (34), and HIV-1 RT (30) by using thiol-reactive azide photocross-linkers. This method is sensitive enough to detect the intramolecular movements associated with normal enzymatic processes carried out by HIV-1 RT. Since neither the introduction of the unique cysteine residue nor their modification with photocross-linking reagents caused significant decrease in the enzymatic activities of RT, we were able to use this model system to investigate interactions between specific points on the fingers domain of RT and DNA template-primer.

The cross-linking data suggest that several positions on the fingers of p66 can interact with the extended template strand. The data imply that the preferred sites of interaction(s) are 5 to 7 bases beyond the polymerase active site. In most cases, binding an incoming dNTP at the polymerase active site decreases the efficiency of cross-linking, suggesting that whatever interactions occur between the fingers of p66 and the extended template involve the "open" configuration of the enzyme in which the fingers move away from the active site rather than the closed configuration with the fingers in direct contact with the incoming dNTP. This makes sense from a structural point of view: in the closed configuration, the template passes over the top of the fingers and would not have ready access to several of the positions (positions 65, 67, and 70) we have modified for this study (25). With the open configuration of HIV-1 RT, there was a strong preference for the cross-linking to the template strand. In the closed conformation, the preference was reduced, particularly for the sites on the protein close to the polymerase active site (positions 65 and 74). This is to be expected if the fingers move toward the active site and the flexibility of the fingers and the template is decreased in the closed conformation.

The decrease in the flexibility of the protein that occurs in the ternary complex could also contribute to a decrease in cross-linking yields. In the closed conformation of the ternary complex, the distance from mutant Cys to the DNA template overhang decreases, but the probability of forming cross-links with suboptimal sites on the DNA template would be lower due to lower flexibility and, therefore, have less contribution to the overall yield. The fact that the yields of cross-linking are increased for the template-primers with a 2-nt extension when ternary complexes are formed, even though the absolute yield of cross-linking is low, provides supporting evidence for the model. A decrease in the amount of cross-linking would also be observed if the distances to all mutant Cys residues from template DNA were increased without a shift in the relative positions of DNA and the Cys residue. If this was true, the BAT-DHP reagent, which has a longer linker, would be less affected by an increase in the distance. Since in our experiments both photocross-linkers produce lower yields in ternary complexes compared to binary ones, the explanation of decreased flexibility in the closed conformation is probably the more likely.

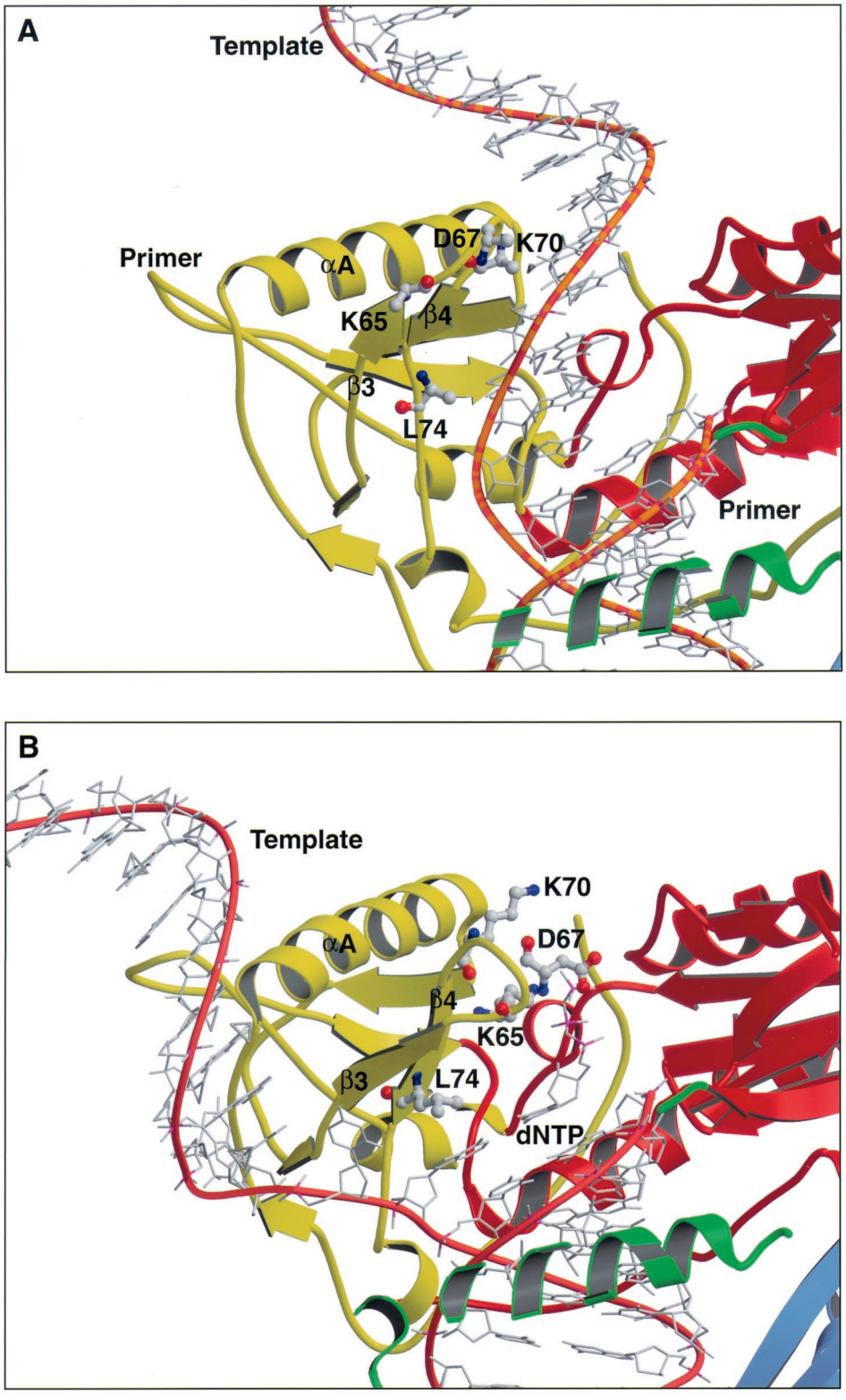

FIG. 7. Models for the extended template in the binary and ternary complexes. This figure (A) is based on the structure determined by Ding et al. (9). It shows the fingers of p66 in yellow with the side chains of L74, K65, D67, and K70 marked. The modeling of the position of the extended template is similar to that of Boyer et al. (5). In the binary complex, the fingers are in the open configuration, giving the extended template the opportunity to interact with amino acids in the β3-β4 loop. (B) Closed configuration (ternary complex) with bound dNTP. The figure is based on the structure determined by Huang et al. (25). In the closed configuration, the β3-β4 loop moves closer to the polymerase active site and closes the dNTP binding pocket. In the structure shown by Huang et al., the extended template passes over the fingers near L74. In the figure, the template was extended based on the portion of the template in the crystal structure. In the figure, the template extension is not in a position where it can easily interact with amino acids at position 65, 67, or 70.

The preferred positions for cross-linking are, for the most part, what would be expected based on models prepared from the "open" binary (RT-DNA) complex. As observed in our experiments with photocross-linking to an extended template, nt +5 to +7 of the template overhang are close enough to have interactions with the mutant cysteines in positions 65 and 74 of the fingers subdomain, and nt +6 to +9 are close to positions 67 and 70. This observation is in good agreement with X-ray data of the binary complex of DNA-RT (9) with template extension modeled in when distances to residues 67, 70, and 65 are measured.

The data for position 74 can be explained by the fact that template residues from +1 to +3 may have their bases turned inside of the helix and away from the cross-linker. This consideration is especially significant for the APTP (nucleophilic) and SH-experiments (S-S bond formation is orientation sensitive and the reactive SH- is on the base). Relative to the APTP, the diazirine cross-linking reagent BATDHP has a longer linker and less preference for reacting with the bases.

The cross-linking data show that the extended template can come quite close to the fingers of p66, but do not define the interactions between the fingers and template. It is possible that there are no specific interactions between the fingers and the template. We attempted to resolve this issue by performing three sets of cross-linking experiments: a specific, selective cross-linking involving the formation of S-S bonds and two types of photocross-linking experiments—one involving a reagent (APTP) that has a moderate reactive half-life and the other involving one (BATDHP) which has an extremely short half-life. All three experiments result in selective cross-linking of protein with the extended template. Not only is there a very high level of S-S cross-linking, but both of the photoactivatable reagents showed substantial cross-linking. In this regard, we believe that the data with BATDHP are probably the most significant, since the half-life of the reactive species is very brief, and it reacts with minimal selectivity. The fact that there is considerable cross-linking with such a nonselective reagent considerably strengthens our belief that the cross-linking depends on a biologically meaningful interaction between the fingers of HIV-1 RT and the extended template. We also think it significant that similar results were obtained with photocross-linking and chemical cross-linking. Although the formation of the S-S bond is chemically selective and specific, Huang et al. (25) showed that for HIV-1 RT, cross-linking of DNA to protein by formation of this type of S-S bond is efficient only when the reactive SH- groups are specifically aligned. As observed in our experiments, differences in cross-linking efficiency for different positions of SH- group along the template extension provide additional confirmation of importance of such alignment.

It is quite clear from the structure of the ternary complex of HIV-1 RT, dsDNA, and incoming dNTP that the fingers of p66 help to form the dNTP binding pocket (25). This does not mean, however, that the fingers have no other role. Furthermore, the fact that the fingers of p66 are intended to help hold the incoming nucleotide appropriately in position at the end of the primer strand means that the tips of the p66 fingers interact with nucleosides and could also interact with DNA. If we consider the position of the fingers tips in the open binary complex (RT-DNA) and extend the template strand along a helical path, then the extended template would be able to contact the fingers 4 to 6 bases beyond the end of the primer. Moreover, by taking a helical path, the extended template would present to the fingers a surface equivalent to that presented by the primer strand (and incoming dNTP) in the closed (ternary) complex. This could explain how the fingers interact with the extended template; however, it still leaves open the question of the significance of this interaction. In this regard, the experiments (5) done to measure the effects of the length of the template extension on the ability of HIV-1 RT to incorporate nucleoside analogs may be important. Although our interpretation of the data has changed, the data have not. The relative sensitivity or resistance of wild-type HIV-1 RT to certain nucleoside analogs is a function of template length: this implies that the extended template has significant interactions with RT, an idea supported by studies that measure the binding of RT to nucleic acid (36). The cross-linking data we present here suggest that such interactions could involve the tips of the fingers of p66. We suggest, based on the cross-linking data (and structural considerations), that, in the open complex, the path that the extended template takes from the polymerase active site first passes near position 74, then passes near 65 and 70, and finally moves past position 67.

What purpose could such interactions serve? HIV-1 RT must be able to copy single-stranded RNAs with secondary structure (presumably in collaboration with nucleocapsid protein [NC]). Moreover, the synthesis of the complete HIV-1 genome requires that the enzyme be capable of synthesis through short regions of double-stranded nucleic acid. Both types of synthesis would require RT (possibly in conjunction with NC) to open up a nucleic acid duplex. If the fingers can interact directly with the extended template, then it is possible that the fingers have an additional role, beyond forming the dNTP binding pocket. The fingers may also prepare the template strand by helping to convert it into a form that has little or no significant secondary structure so that it can be easily and efficiently copied.

ACKNOWLEDGMENTS

We thank Edward Wu for helpful assistance in molecular model graphic presentation and Hilda Marusiodis for help in manuscript preparation.

This research was supported in part by the NCI, NIDDK, and NIGMS.

REFERENCES

1. **Allerson, C. R., and G. L. Verdine.** 1995. Synthesis and biochemical evaluation of RNA containing an intrahelical disulfide crosslink. Chem. Biol. **2:**667–675.
2. **Benn, S., R. Rutledge, T. Folks, J. Gold, L. Baker, J. McCormick, P. Feorino, P. Piot, T. Quinn, and M. Martin.** 1985. Genomic heterogeneity of AIDS retroviral isolates from North America and Zaire. Science **230:**949–951.
3. **Boyer, P. L., J. Ding, E. Arnold, and S. H. Hughes.** 1994. Subunit specificity of mutations that confer resistance to nonnucleoside inhibitors in human immunodeficiency virus type 1 reverse transcriptase. Antimicrob. Agents Chemother. **38:**1909–1914.
4. **Boyer, P. L., A. L. Ferris, and S. H. Hughes.** 1992. Cassette mutagenesis of the reverse transcriptase of human immunodeficiency virus type 1. J. Virol. **66:**1031–1039.
5. **Boyer, P. L., C. Tantillo, A. Jacobo-Molina, R. G. Nanni, J. Ding, E. Arnold, and S. H. Hughes.** 1994. Sensitivity of wild-type human immunodeficiency virus type 1 reverse transcriptase to dideoxynucleotides depends on template length: the sensitivity of drug-resistant mutants does not. Proc. Natl. Acad. Sci. USA **91:**4882–4886.
6. **Coffin, J. M., S. H. Hughes, and H. E. Varmus.** 1997. Retroviruses. Cold Spring Harbor Laboratory Press, Plainview, N.Y.

7. **Custer, L., B. Zajc, J. M. Sayer, C. Cullinane, D. R. Phillips, A. M. Cheh, D. M. Jerina, V. A. Bohr, and S. J. Mazur.** 1999. Stereospecific differences in repair by human cell extracts of synthesized oligonucleotides containing trans-opened 7, 8, 9, 10-tetrahydrobenzo[a]pyrene 7,8-diol 9,10-epoxide N2-dG adduct stereoisomers located within the human K-ras codon 12 sequence. Biochemistry **38:**569–581.
8. **Das, K., J. Ding, Y. Hsiou, A. D. Clark, Jr., H. Moereels, L. Koymans, K. Andries, R. Pauwels, P. A. Janssen, P. L. Boyer, P. Clark, R. H. Smith, Jr., M. B. Kroeger Smith, C. J. Michejda, S. H. Hughes, and E. Arnold.** 1996. Crystal structures of 8-Cl and 9-Cl TIBO complexed with wild-type HIV-1 RT and 8-Cl TIBO complexed with the Tyr181Cys HIV-1 RT drug-resistant mutant. J. Mol. Biol. **264:**1085–1100.
9. **Ding, J., K. Das, Y. Hsiou, S. G. Sarafianos, A. D. Clark, Jr., A. Jacobo-Molina, C. Tantillo, S. H. Hughes, and E. Arnold.** 1998. Structure and functional implications of the polymerase active site region in a complex of HIV-1 RT with a double-stranded DNA template-primer and an antibody Fab fragment at 2.8 A resolution. J. Mol. Biol. **284:**1095–1111.
10. **Ding, J., K. Das, H. Moereels, L. Koymans, K. Andries, P. A. Janssen, S. H. Hughes, and E. Arnold.** 1995. Structure of HIV-1 RT/TIBO R 86183 complex reveals similarity in the binding of diverse nonnucleoside inhibitors. Nat. Struct. Biol. **2:**407–415.
11. **Ding, J., S. H. Hughes, and E. Arnold.** 1997. Protein-nucleic acid interactions and DNA conformation in a complex of human immunodeficiency virus type 1 reverse transcriptase with a double-stranded DNA template-primer. Biopolymers **44:**125–138.
12. **Dirscherl, W., and F. W. Weingarten.** 1951. Justus Liebigs. Ann. Chem. **574:**131–139.
13. **Dumoulin, P., R. H. Ebright, R. Knegtel, R. Kaptein, M. Granger-Schnarr, and M. Schnarr.** 1996. Structure of the LexA repressor-DNA complex probed by affinity cleavage and affinity photo-cross-linking. Biochemistry **35:**4279–4286.
14. **Dumoulin, P., P. Oertel-Buchheit, M. Granger-Schnarr, and M. Schnarr.** 1993. Orientation of the LexA DNA-binding motif on operator DNA as inferred from cysteine-mediated phenyl azide crosslinking. Proc. Natl. Acad. Sci. USA **90:**2030–2034.
15. **Erlanson, D. A., L. Chen, and G. L. Verdine.** 1993. Allosteric effects on enzyme action in disulfide-crosslinked DNA. J. Am. Chem. Soc. **115:**12583–12584.
16. **Esnouf, R. M., J. Ren, A. L. Hopkins, C. K. Ross, E. Y. Jones, D. K. Stammers, and D. I. Stuart.** 1997. Unique features in the structure of the complex between HIV-1 reverse transcriptase and the bis(heteroaryl)piperazine (BHAP) U-90152 explain resistance mutations for this nonnucleoside inhibitor. Proc. Natl. Acad. Sci. USA **94:**3984–3989.
17. **Evans, B. J., J. T. Doi, and W. K. Musker.** 1990. Kinetics of aqueous periodate oxidation of aliphatic disulfides and thioesters. J. Org. Chem. **55:**5280–5286.
18. **Favre, A., C. Saintome, J. L. Fourrey, P. Clivio, and P. Laugaa.** 1998. Thionucleobases as intrinsic photoaffinity probes of nucleic acid structure and nucleic acid-protein interactions. J. Photochem. Photobiol. **42:**109–124.
19. **Gao, H. Q., P. L. Boyer, S. G. Sarafianos, E. Arnold, and S. H. Hughes.** 2000. The role of steric hindrance in 3TC resistance of human immunodeficiency virus type-1 reverse transcriptase. J. Mol. Biol. **300:**403–418.
20. **Gao, H. Q., S. G. Sarafianos, E. Arnold, and S. H. Hughes.** 1999. Similarities and differences in the RNase H activities of human immunodeficiency virus type 1 reverse transcriptase and Moloney murine leukemia virus reverse transcriptase. J. Mol. Biol. **294:**1097–1113.
21. **Hopkins, A. L., J. Ren, R. M. Esnouf, B. E. Willcox, E. Y. Jones, C. Ross, T. Miyasaka, R. T. Walker, H. Tanaka, D. K. Stammers, and D. I. Stuart.** 1996. Complexes of HIV-1 reverse transcriptase with inhibitors of the HEPT series reveal conformational changes relevant to the design of potent non-nucleoside inhibitors. J. Med. Chem. **39:**1589–1600.
22. **Hopkins, A. L., J. Ren, H. Tanaka, M. Baba, M. Okamato, D. I. Stuart, and D. K. Stammers.** 1999. Design of MKC-442 (emivirine) analogues with improved activity against drug-resistant HIV mutants. J. Med. Chem. **42:**4500–4505.
23. **Hsiou, Y., K. Das, J. Ding, A. D. Clark, Jr., J. P. Kleim, M. Rosner, I. Winkler, G. Riess, S. H. Hughes, and E. Arnold.** 1998. Structures of Tyr188Leu mutant and wild-type HIV-1 reverse transcriptase complexed with the non-nucleoside inhibitor HBY 097: inhibitor flexibility is a useful design feature for reducing drug resistance. J. Mol. Biol. **284:**313–323.
24. **Hsiou, Y., J. Ding, K. Das, A. D. Clark, Jr., S. H. Hughes, and E. Arnold.** 1996. Structure of unliganded HIV-1 reverse transcriptase at 2.7 A resolution: implications of conformational changes for polymerization and inhibition mechanisms. Structure **4:**853–860.
25. **Huang, H., R. Chopra, G. L. Verdine, and S. C. Harrison.** 1998. Structure of a covalently trapped catalytic complex of HIV-1 reverse transcriptase: implications for drug resistance. Science **282:**1669–1675.
26. **Jacobo-Molina, A., J. Ding, R. G. Nanni, A. D. Clark, Jr., X. Lu, C. Tantillo, R. L. Williams, G. Kamer, A. L. Ferris, P. Clark, A. Hizi, S. H. Hughes, and E. Arnold.** 1993. Crystal structure of human immunodeficiency virus type 1 reverse transcriptase complexed with double-stranded DNA at 3.0 A resolution shows bent DNA. Proc. Natl. Acad. Sci. USA **90:**6320–6324.
27. **Katlama, C.** 1999. Review of NNRTIs: 'today and tomorrow.' Int. J. Clin. Pract. Suppl. **103:**16–20.
28. **Kohlstaedt, L. A., J. Wang, J. M. Friedman, P. A. Rice, and T. A. Steitz.** 1992. Crystal structure at 3.5 A resolution of HIV-1 reverse transcriptase complexed with an inhibitor. Science **256:**1783–1790.
29. **Moreland, R. B., P. K. Smith, E. K. Fujimoto, and M. E. Dockter.** 1982. Synthesis and characterization of *N*-(4-azidophenylthio)phthalimide: a cleavable, photoactivable crosslinking reagent that reacts with sulfhydryl groups. Anal. Biochem. **121:**321–326.
30. **Rausch, J. W., B. K. Sathyanarayana, M. K. Bona, and S. F. Le Grice.** 2000. Probing contacts between the ribonuclease H domain of HIV-1 reverse transcriptase and nucleic acid by site-specific photocross-linking. J. Biol. Chem. **275:**16015–16022.
31. **Ren, J., R. Esnouf, A. Hopkins, C. Ross, Y. Jones, D. Stammers, and D. Stuart.** 1995. The structure of HIV-1 reverse transcriptase complexed with 9-chloro-TIBO: lessons for inhibitor design. Structure **3:**915–926.
32. **Ren, J., C. Nichols, L. E. Bird, T. Fujiwara, H. Sugimoto, D. I. Stuart, and D. K. Stammers.** 2000. Binding of the second generation non-nucleoside inhibitor S-1153 to HIV-1 reverse transcriptase involves extensive main chain hydrogen bonding. J. Biol. Chem. **275:**14316–14320.
33. **Rodgers, D. W., S. J. Gamblin, B. A. Harris, S. Ray, J. S. Culp, B. Hellmig, D. J. Woolf, C. Debouck, and S. C. Harrison.** 1995. The structure of unliganded reverse transcriptase from the human immunodeficiency virus type 1. Proc. Natl. Acad. Sci. USA **92:**1222–1226.
34. **Spanggord, R. J., and P. A. Beal.** 2000. Site-specific modification and RNA crosslinking of the RNA-binding domain of PKR. Nucleic Acids Res. **28:**1899–1905.
35. **Tate, J. J., J. Persinger, and B. Bartholomew.** 1998. Survey of four different photoreactive moieties for DNA photoaffinity labeling of yeast RNA polymerase III transcription complexes. Nucleic Acids Res. **26:**1421–1426.
36. **Tong, W., C. D. Lu, S. K. Sharma, S. Matsuura, A. G. So, and W. A. Scott.** 1997. Nucleotide-induced stable complex formation by HIV-1 reverse transcriptase. Biochemistry **36:**5749–5757.
37. **Varmus, H.** 1988. Retroviruses. Science **240:**1427–1435.
38. **Weber, P. J., and A. G. Beck-Sickinger.** 1997. Comparison of the photochemical behavior of four different photoactivatable probes. J. Pept. Res. **49:**375–383.
39. **Weiss, R. A., N. Teich, H. Varmus, and J. Coffin.** 1985. RNA tumor viruses, 2nd ed. Cold Spring Harbor Laboratory Press, Plainview, N.Y.